Biophysical Journal Volume 68 March 1995 925–935

Quantal Transmission at Purinergic Junctions: Stochastic Interaction between ATP and its Receptors

M. R. Bennett, L. Farnell, W. G. Gibson, and S. Karunanithi

The Neurobiology Laboratory, Department of Physiology and The School of Mathematics and Statistics, University of Sydney, N.S.W. 2006, Australia

ABSTRACT The time course of most quantal currents recorded with a small diameter electrode placed over visualized varicosities of sympathetic nerve terminals that secrete ATP was determined: these had a time to reach 90% of peak of 1.3–1.8 ms and a time constant of decay of 12–18 ms; they were unaffected by blocking ectoenzymes or the uptake of adenosine. Monte Carlo methods were used to analyze the stochastic interaction between ATP, released in a packet from a varicosity, and the underlying patch of purinoceptors, to reconstitute the time course of the quantal current. This leads to certain restrictions on the possible number of ATP molecules in a quantum (about 1000) and the density of purinoceptors at the junctions (about 1000 μm^{-1}), given the known geometry of the junction and the kinetics of ATP action. The observed quantal current has a relatively small variability (coefficient of variation <0.1), and this stochastic property is reproduced for a given quantum of ATP. Potentiation effects (of about 12%) occur if two quanta are released from the same varicosity because the receptor patch is not saturated even by the release of two quanta. The simulations show that quantal currents have a characteristically distinct shape for varicosities with different junctional cleft widths (50–200 nm). Finally, incorporation of an ectoenzyme with the known kinetics of ATPase into the junctional cleft allows for a quantal current of the observed time course, provided the number of ATP molecules in a quantum is increased over the number in the absence of the ATPase.

INTRODUCTION

ATP is a transmitter at autonomic neuromuscular junctions (Burnstock, 1982) and synapses (Evans et al., 1992; Silinsky et al., 1992) as well as in the central nervous system (Edwards et al., 1992; for review, see Edwards and Gibb, 1993). The time course of the spontaneous synaptic currents at these purinergic junctions and synapses is so fast as to suggest that they are due to direct gating of channels without involving second messengers. These ATP-activated channels are cation-specific, some showing a specificity for calcium over other cations (as in vascular smooth muscle, Benham and Tsien, 1987), whereas others show the reverse (as in sensory neurones, Bean et al., 1990). The single-channel chord conductance to exogenous ATP is 1–5 pS in smooth muscle in the presence of quasi-physiological ionic conditions and about 10 pS in divalent-free solutions (Friel, 1988; Benham and Tsien, 1987). In cardiac atrial cells, the unitary conductances are at least an order of magnitude smaller (Friel and Bean, 1988). Currents due to the spontaneous release of ATP on arterioles are generated by a conductance change of about 1.5–3 nS (Finkel et al., 1984); if the junctional purinoceptors have the same conductance as the extrajunctional purinoceptors (1–5 pS), then these unitary currents are due to the activation of between 300 and 3000 receptors. At the autonomic neuromuscular junction, varicosities that make close contacts with smooth muscle cells do so over an area of close apposition between prejunctional and postjunctional membranes; this area is approximately 0.4 μm^2, and the separation is about 50 nm or more (Bennett, 1994). The junctional current due to a quantum of ATP reaches 90% of its peak value in a few milliseconds and then declines exponentially with a single time constant of 10–20 ms (see Results). The dose-response curve for the ATP-generated currents at extrajunctional purinoceptors are best-fitted by a kinetic equation based on ATP binding cooperatively at two sites on the purinoceptor for ligand-gated channel opening (Friel, 1988; Friel and Bean, 1988). The question arises whether these constraints on the number of activated receptors, the geometry of the junction and the time course of the quantal currents, together with the kinetic description of the interaction of ATP with its receptors, can be accommodated within a consistent model of purinergic quantal transmission.

The quantal event at the somatic neuromuscular junction has been reconstructed previously using a set of differential equations based on a model in which, after the sudden appearance of acetylcholine in the synaptic cleft, there is radial diffusion of the transmitter, enzymatic hydrolysis by acetylcholinesterase, and binding to the receptors (Wathey et al., 1979; Parnas et al., 1989). An alternative approach, using Monte Carlo methods, allows for details of the history of individual molecules of acetylcholine to be followed after their secretion in a quantum (Bartol et al., 1991). In both cases, the time course of the quantal current could be reconstructed from the known geometry of the somatic neuromuscular junction, the density of nicotinic receptors (Salpeter and Eldefrawi, 1973), the number of acetylcholine molecules in a quantum (Kuffler and Yoshikami, 1975), and the stoichiometry of the reaction between acetylcholine and its receptors together with the binding constants (Land et al., 1984; Dionne et al., 1978; Chabala et al., 1986; Colquhoun and Ogden, 1988). Very few of the equivalent parameters are

Received for publication 29 August 1994 and in final form 6 December 1994.

Address reprint requests to Professor Max Bennett, Neurobiology Laboratory F13, University of Sydney, N.S.W. 2006, Australia. Tel.: 61-2-692-2034; Fax: 61-2-692-4740; E-mail: gibson_w@maths.su.oz.au.

0006-3495/95/03/925/11 $2.00

known for the purinergic junctions. Therefore, we have used Monte Carlo procedures to determine appropriate values for these unknown parameters, which will generate the purinergic quantal event at autonomic neuromuscular junctions.

MATERIALS AND METHODS

Experimental method

The vas deferens of mice (strain Balb/c), 5–6 weeks old, were used in these experiments. Animals were anesthetised with halothane and then killed by a cervical fracture. An incision was made into the lower abdomen, and both vas deferens and connective tissue containing the fine hypogastric nerves were dissected free. Careful stripping of the sheath of epimysium from the surface of the vas deferens was then performed by gently teasing the sheath from the prostatic end for a distance of about 5 mm along the vas deferens. The tissue was then placed in a Perspex chamber of 3-ml capacity and pinned through the epididymal end to a sheet of sylgard at the bottom of the chamber. The bathing solution had the following composition (mM): Na^+, 136.9; K^+, 4.0; Mg^{2+}, 1.0; Cl^-, 127.1–129.1; $(H_2PO_4)^-$, 1.5; $(HCO_3)^-$, 16.3; Ca^{2+}, 1.0–2.0; and glucose, 7.77. The solution was gassed continuously with 95% O_2 so that the pH was maintained between 7.1 and 7.4. The tissue was perfused with warm (33°C) modified Tyrode solution at the rate of 2–4 ml/min.

The vas deferens was perfused for 40 s with 3-3-dithyloxardicarbocyanine iodide ($DiOC_2(5)$, 0.05–0.5 μM) and then washed in modified Tyrode solution for 5 min (Bennett et al., 1986). $DiOC_2(5)$ fluorescence of the axons and varicosities was observed during excitation at 540 nm using an Olympus rhodamine filter set (Olympus, BH-2 microscope). Preparations were viewed using a 50× long working distance objective (Olympus, ULWD-MS Plan 50). The adverse effects of $DiOC_2(5)$ and fluorescence on quantal secretions have been studied previously (Bennett et al., 1986). The concentration of $DiOC_2(5)$ was kept to less than 0.5 μM and the period of excitation to less than 2 min to minimize any adverse effects of $DiOC_2(5)$ excitation. The field of excitation was restricted to the region being examined, and the field of fluorescing varicose axons was hand-drawn on the TV monitor screen as soon as their fluorescent profiles had been identified; excitation was then terminated, and transmitted light was used to view the same area. Structures such as blood vessels and connective tissue were then drawn onto the TV monitor; the glass microelectrode was then moved into the field of the drawing of the varicose axons. Any shift of the varicose axons with respect to the drawing could finally be checked by refluorescing the varicose axons at the termination of the experiment. It has already been shown that a 5-μm lateral movement of the microelectrode away from a varicosity results in complete loss of the spontaneous excitatory junction potential (Lavidis Bennett, 1992). Electrophysiological study was only made of the fluorescing varicose axons on the surface of the muscle, which were at least 10 μm distant from any other surface axon. Recording microelectrodes filled with modified Tyrode solution, and having a tip diameter of 3–4 μm, were placed over single visualized varicosities. Both evoked excitatory junctional currents (EJCs) and SEJCs were recorded and stored on hard disk using a Macintosh IIci computer and MacLab software. Drugs used were the ectoenzyme 5′-nucleotidase inhibitor, α,β-methylene - ADP (AOPCP; Burger and Lowenstein, 1970) (Sigma Chemical Co., St. Louis, MO) and the purine uptake blocker, dipyridamole (Wu Phillis, 1984) (Boehringer Ingelheim, Germany).

Monte Carlo simulation method

The kinetics of ATP interaction with extrajunctional receptors is governed by

$$2A + R \underset{k-1}{\overset{2k_1}{\rightleftarrows}} A + AR \underset{2k-2}{\overset{k_2}{\rightleftarrows}} A_2R' \underset{\alpha}{\overset{\beta}{\rightleftarrows}} A_2R^*, \quad (1)$$

where A is an ATP molecule, R is a receptor molecule containing two binding sites, AR is the singly bound molecule, A_2R', is the doubly bound molecule in the closed conformation, and A_2R^* is the doubly bound molecule in the open conformation, corresponding to an open channel. In practice (cf. Bartol et al., 1991), Eq. 1 can be simplified to

$$2A + R \underset{k-1}{\overset{2k_1}{\rightleftarrows}} A + AR \underset{2k_{eff}}{\overset{k_2}{\rightleftarrows}} A_2R, \quad (2)$$

where $k_{eff} = (\alpha/(\alpha + \beta))k_{-2}$ and the number of open states (A_2R^*) is found by multiplying the number of doubly bound states (A_2R) by $\beta/(\alpha + \beta)$. Note that A_2R signifies *all* doubly bound states; that is, it includes the closed state A_2R' and the open state A_2R^*. If an ectoenzyme such as ATPase is present, then the above equations need to be supplemented by

$$A + E \overset{k_3}{\rightarrow} EA, \quad (3)$$

$$EA \overset{k_4}{\rightarrow} E + P, \quad (4)$$

where E denotes the ectoenzyme and P denotes the final products of hydrolysis.

To the above kinetic scheme must be added the spatial and temporal diffusion of the ATP molecules after quantal release. The Monte Carlo method involves following the motion of each molecule as it executes a random walk in free space, is reflected from presynaptic and postsynaptic membranes, and binds to or unbinds from receptor molecules. A detailed description and justification of the Monte Carlo method, as applied to the release of ACh in the neuromuscular junction, has been given by Bartol et al. (1991). The present calculations closely follow their methods. The principal difference is in the geometry of the system, which is here simplified to consist of two flat plates, usually taken to be 50 nm apart, and shaped as squares of side 5 μm as shown in Fig. 1. Receptors are found only in small patches in the center of the postsynaptic membrane, modeled as squares usually of edge 0.64 μm (giving an area of 0.4 μm^2). These squares are subdivided into tiles of appropriate size, depending on the assumed receptor density, each tile containing one receptor. The actual size of the receptor is 10 nm^2, which is much smaller than the tile size. It is not known if ectoenzymes such as ATPase are localized at autonomic neuromuscular junctions in much the same way as acetylcholinesterase is at the somatic neuromuscular junction. In the absence of such knowledge, the model of Bartol et al. (1991) has been followed, and the enzyme has been located in a plane midway between the varicosity and muscle membranes and occupying an area the same as that of the receptors (Fig. 1).

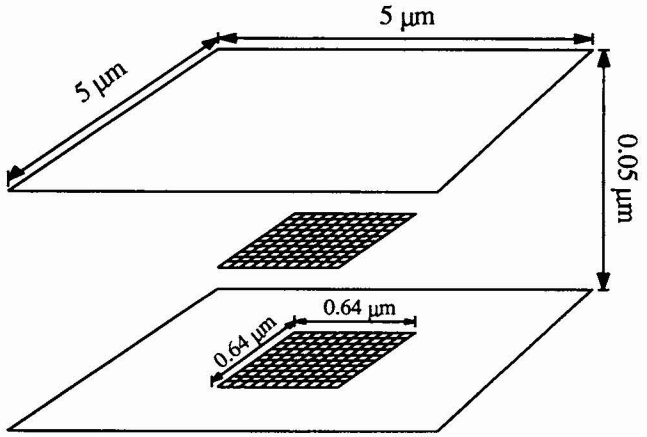

FIGURE 1 Diagrammatic representation (not to scale) of a junction between a sympathetic varicosity membrane and a smooth muscle cell membrane, separated by 50 nm. The lower hatched area represents the P_{2x}-receptor patch, which is taken to be square of side 0.64 μm. The upper hatched area represents the ectoenzymes, if these are present, midway between pre- and postjunctional membranes. Transmitter is released onto the center of the receptor patch. Although the varicosity membrane is likely to extend for only about 2 μm × 1 μm, it has been taken here to cover 5 μm^2 to simplify the calculations.

Quanta of ATP are secreted at time $t = 0$ from the presynaptic membrane at one or more points directly opposite the centers of the receptor patches. Each molecule is moved randomly, using a timestep of 0.75 μs, for a total of 60 ms. The algorithms and formulas used are as described by Bartol et al. (1991).

Choice of kinetic rate constants for the simulation

Equation 2 for the effective kinetics of ATP binding involves four rate parameters, k_1, k_{-1}, k_2, k_{eff}, and the ratio α/β. The forward rate of the first step can be fixed by assuming that it is the same as for the triple-binding case at purinergic synapses (Bean, 1990); thus, $k_1 = k_{on} = 1.2 \times 10^7\ M^{-1}\ s^{-1}$. The dissociation constants k_{-1} and k_{eff} largely determine the decay time of the junctional current, about 13 ms (see below). In the absence of any evidence for cooperativity in unbinding, the choice $k_{-1} = k_{eff} = 80\ s^{-1}$ was made. Bean (1990) gives the value $\alpha/\beta = 4$; in the present calculations, this was changed slightly to $\alpha/\beta = 3$ to ensure a sufficient number of open channels (see below). The remaining rate constant, k_2, can be fixed by appeal to the concentration-response curve. From Eq. 3 the equilibrium current I is given by

$$\frac{I}{I_\infty} = \frac{1}{1 + 2K_{eff}/[A] + K K_{eff}/[A]^2}, \quad (5)$$

where $[A]$ is the ATP concentration and I_∞ is the current at infinite concentration. K and K_{eff} are the microscopic dissociation constants defined by $K = k_{-1}/k_1$ and $K_{eff} = k_{eff}/k_2$. From the values given above, $K = 6.67\ \mu M$ and the choice $K_{eff} = K/5$ then gives good agreement between Eq. 4 and the concentration-response curve for smooth muscle (Friel, 1988, his Fig. 3), as shown in Fig. 2. Thus, $k_2 = 6.0 \times 10^7\ M^{-1}\ s^{-1} = 5k_1$, and there is a cooperativity of 5 in the second binding over the first. The kinetic parameters have thus been determined by using the basic forward binding rate of Bean (1990) for the first binding, the known decay time to fix the dissociation rates, and the experimental concentration-response curve of Friel (1988) to fix the second binding rate. These parameter values are used on the basis that the receptor properties studied by Friel (1988) and Bean (1990) are applicable to junctional receptors. A further parameter is the diffusion coefficient D, and the value $D = 3 \times 10^{-6}\ cm^2\ s^{-1}$ given by Wathey et al. (1979) for acetylcholine has been used. This may be an overestimate because ATP has a higher molecular weight than acetylcholine and also three negatively charged phosphate groups. However, a linear least-squares fit to a log-log plot of diffusion coefficients versus molecular weight for a number of large protein molecules in water at 20°C gave an estimate of $4 \times 10^{-6}\ cm^2\ s^{-1}$ for ATP. (The same fit gave $6 \times 10^{-6}\ cm^2\ s^{-1}$ for acetylcholine; this latter value is very close to the choice of Bartol et al., namely, $6.5 \times 10^{-6}\ cm^2\ s^{-1}$.) To test the effect of a much slower diffusion rate, some runs were also done for $D = 1 \times 10^{-6}\ cm^2\ s^{-1}$.

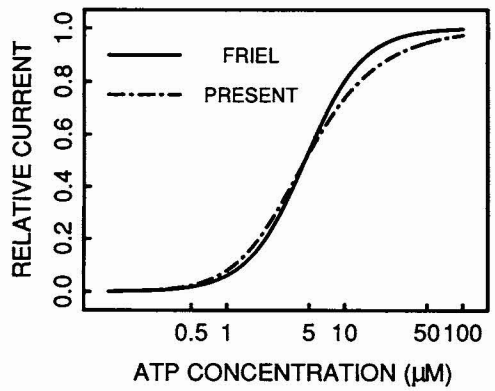

FIGURE 2 Concentration dependence of the peak ATP-induced current. The solid curve is Friel's fit to his experimental data (Friel, 1988; Fig. 3); the broken curve comes from Eq. 4 with the parameter choice $K = 6.67\ \mu M$ and $K_{eff} = K/5$.

The hydrolysis of ATP has a $K_m = k_4/k_3$ of 300 μM for cultured endothelial cells (Gordon et al., 1986). Using this K_m and guided by the values of k_3 and k_4 for acetylcholinesterase (Wathey et al., 1979; Bartol et al., 1991), the choice $k_3 = 5.33 \times 10^7\ M^{-1}\ s^{-1}$ and $k_4 = 1.6 \times 10^4\ s^{-1}$ has been made.

RESULTS

Experimental characteristics of the quantal current

SEJCs were recorded from visualized varicosities on the surface of the mouse vas deferens with 2–3 μm diameter extracellular recording microelectrodes (Fig. 3). Amplitude-frequency histograms for these SEJCs were typically skewed (Fig. 4 *A*), which might be due to multiquantal releases (Bennett, 1994). The frequency histograms of the time for the SEJC to reach within 90% of the peak value were not Gaussian, but tended to follow a gamma distribution with mode at 1.4 to 1.8 ms (mean ± SD of 2.23 ± 0.08 ms; Fig. 4 *B*). SEJCs with long times to peak (>2 ms) all belonged to amplitudes around the principal mode of the amplitude-frequency histogram at about 35 μV (Fig. 5 *A*). The frequency histograms of the time constant for exponential decay of the SEJCs also tended to follow a gamma distribution with a mode at 12 to 18 ms (22 ± 1.2 ms; Fig. 4 *C*). Again, the long decay times were all grouped around the principal mode of the amplitude-frequency histogram at about 35 μV (Fig. 5 *B*).

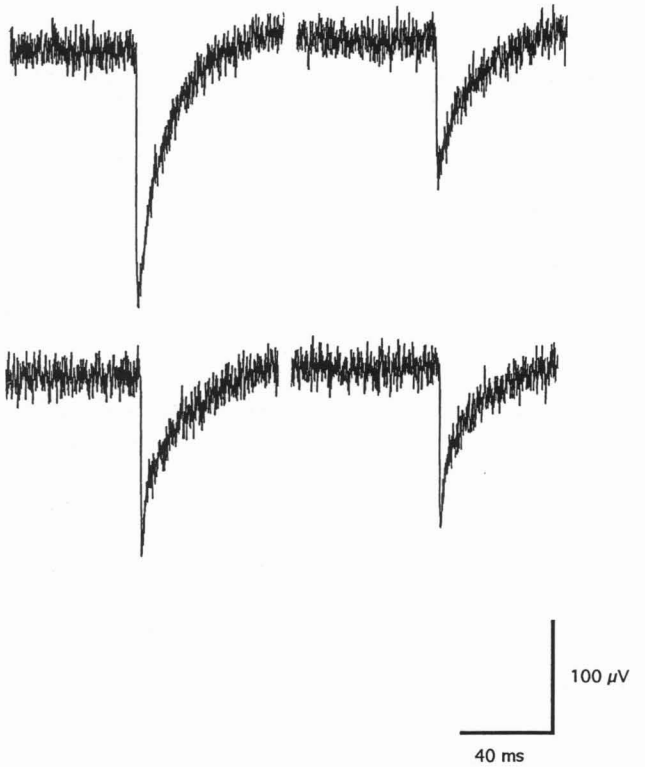

FIGURE 3 SEJCs recorded with a 3-μm extracellular electrode placed over a visualized varicosity on the surface of the mouse vas deferens; the average time course of rise of these (10–90%) is 1.6 ms, and the decline occurs approximately exponentially with a time constant of 16 ms.

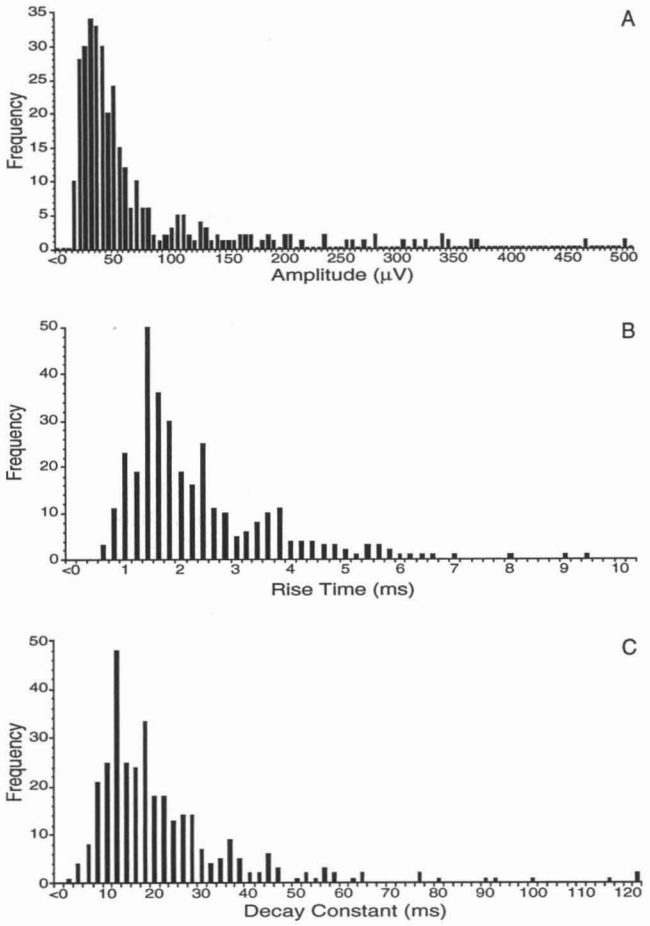

FIGURE 4 Characteristics of the SEJC (or quantal current). (*A*) Amplitude-frequency histogram of SEJCs (63 ± 4 μV is mean ± SEM); (*B*) frequency histogram of the times to reach 90% of the peak current (2.23 ± 0.08 ms; modal value 1.3–1.8 ms). (*C*) Frequency histogram of the time constant of exponential decay of the SEJC (22 ± 1.2 ms; modal value 12–18 ms). Results are pooled for four recordings, each with 3-μm diameter electrodes.

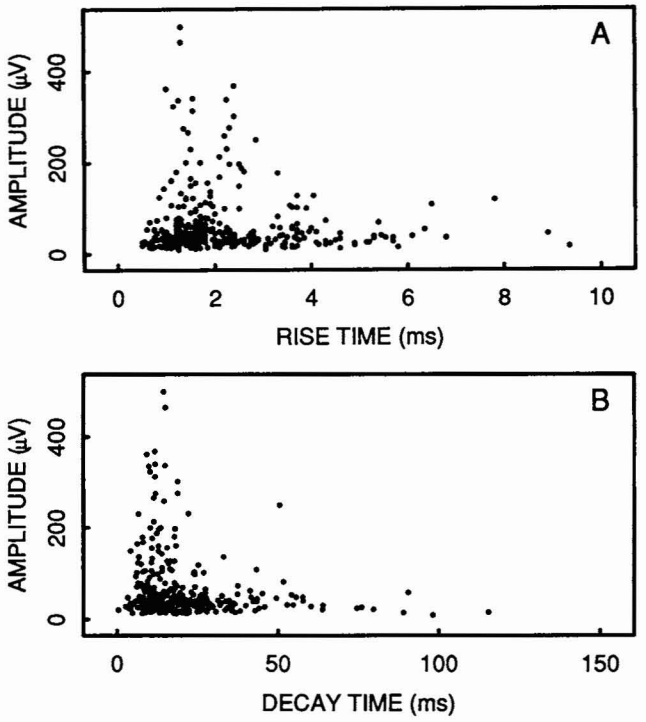

FIGURE 5 Relationship between the amplitude of SEJCs and their rise time to 90% (*A*) and their time constant of decay (*B*). Results as for Fig. 4. Note that the modal values of the 90% rise time and time constant of decay in Fig. 4 occur for a wide range of different SEJC amplitudes.

The transmitter ATP, acting on P_{2x} purinoceptors at these junctions (Sneddon and Burnstock, 1984; Sneddon and Westfall, 1984), may be inactivated because of hydrolysis by ectoenzymes (Nagy, 1986). This may require hydrolysis of ADP to adenosine by 5′-nucleotidase to block the effects of endogenous agonists on these receptors because both ADP and ATP are equally effective at suramin-blocked purinoceptors (Dubyak El-Moatassim, 1993). Inhibition of this ectoenzyme by AOPCP (50 μM) did not affect the time course or amplitude-frequency histograms of SEJCs in four experiments. The adenosine uptake blocker dipyridamole (1 μM) also had no effect on the SEJC. Addition of both AOPCP and dipyridamole together did not affect the characteristics of the SEJC. These results suggest that an ATPase is not contributing to the time course of the EJC, and consideration of such a possibility, therefore, is left to the last section below.

Reconstruction of the quantal current

Close regions of apposition between varicosities and smooth muscle cells at purinergic neuromuscular junctions are about 50 nm wide (see, e.g., Klemm, 1993; Hirst et al., 1992). At this distance, only a single basal lamina is intercalated between the presynaptic varicosity membrane and the postsynaptic smooth muscle cell.

The time course of the quantal event can be reconstituted if a vesicle secretes 1000 molecules onto a receptor density of 1000 μm^{-2}. Fig. 6 *A* shows that the number of free ATP molecules in the receptor region declines rapidly over about 20 ms, primarily due to the diffusion of the molecules away from the receptors and, to a much lesser extent, the binding of the molecules to the receptors. Fig. 6 *B* shows the time course of change in the number of open channels (A_2R^*), as well as that of singly bound (AR) and doubly bound (A_2R) channels, under these conditions. The number of open channels increases to 90% of the maximum in 1.4 ± 0.3 ms and then declines exponentially with a time constant of 13 ± 2 ms (Fig. 6 *B*). The choice of values for the number of ATP molecules in a vesicle and for the receptor density is constrained by the geometry of the junction as well as by the known stoichiometry of the kinetic reaction and time course of the quantal event. Fig. 7 shows the dependence of the 90% rise time (Fig. 7 *A*) and number of open channels (Fig. 7 *B*) on the number of ATP molecules secreted [ATP] for different receptor densities. As the value of [ATP] increases, the 90% rise time gradually decreases or remains approximately constant at very high densities (Fig. 7 *A*), whereas the number of open channels increases (Fig. 7 *B*). There is only a narrow range of values of [ATP] and of

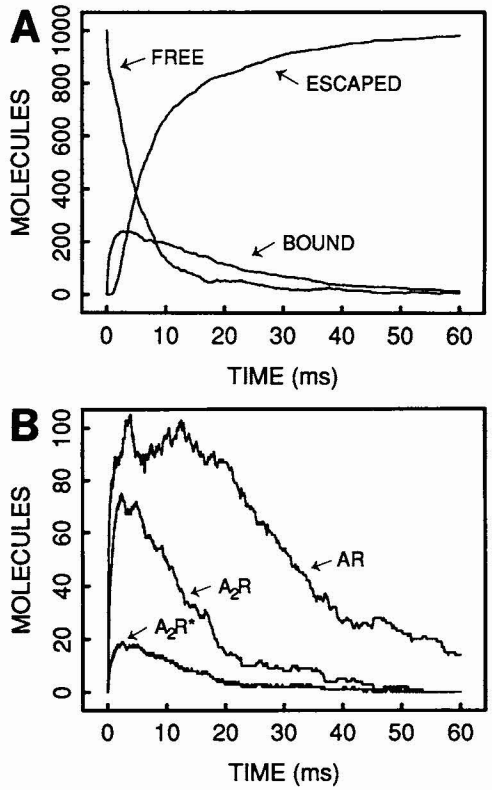

FIGURE 6 Time course of purinergic quantal transmission. 1000 ATP molecules are released at time $t = 0$ from a point 50 nm above the center of a square receptor patch of area 0.4 μm^2 containing a uniform distribution of receptors of density 1000 μm^{-2}. (*A*) The time course of bound ATP, as well as the number of free ATP molecules and the number that escape from the junctional cleft. (*B*) The time course of single-bound receptors (*AR*), doubly bound receptors, (A_2R), and open channels (A_2R^*).

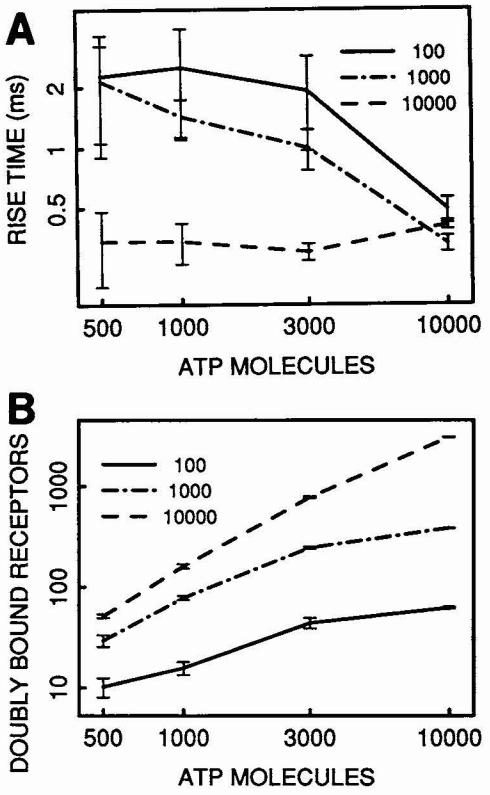

FIGURE 7 Dependence of rise time and number of open channels on quantal size. (*A*) On a log-log scale, the change in the time to reach 90% of maximum A_2R with an increase in the ATP content of a quantum for three receptor densities (100 μm^{-2} ——; 1,000 μm^{-2} – . – . –; 10,000 μm^{-2} – – –). The error bars show 1 SD to each side of the mean. (*B*) The increase in the maximum number of doubly bound receptors (A_2R) with an increase in the ATP content of a quantum for three receptor densities (as in *A*); again, the error bars show 1 SD from the mean. The maximum number of open channels is one-quarter of the maximum number of A_2R molecules.

receptor density that will give a 1.4-ms rise time and also a reasonable number of A_2R^*. The number of A_2R^* needs to be at least about 20 to ensure that quantal currents do not clearly show individual channel openings and closings on their rising and falling phases; this requires an A_2R of at least 80, based on $\alpha/\beta = 3$. These constraints lead to values of [ATP] of 1000 and a receptor density of 1000 μm^{-2}. The exponential decline of A_2R is determined mainly by the reverse rate constants (see Materials and Methods), and so these values can be fixed to give a time constant of decay of 13 ms. Under these conditions, the quantal event (A_2R^*) of Fig. 6 *B* is obtained.

Because it is possible that the diffusion of ATP is slower than is indicated solely by its molecular weight, some calculations were also done with $D = 1 \times 10^{-6}$ cm^2 s^{-1}. The effect was to increase the peak number of open channels and also to increase the decay time. Both of these effects can be compensated for by increasing the dissociation constants, so the overall conclusions are not changed.

Stochastic properties of quantal transmitter-receptor interaction during the quantal current

One component of quantal variability arises from the stochastic properties of receptor-transmitter interactions (Faber et al., 1992). Such variability at the purinergic junction is computed in Fig. 8 *A*, which shows the results of 10 different runs using the same parameters as those for Fig. 6 *B*. The mean of 10 different runs, together with upper and lower bounds 1 SD from the mean, is shown in Fig. 8 *B*, and the SD alone is shown in Fig. 8 *C*. The results indicate that the SD increases and decreases rapidly during the rising phase of the quantal event and then rises slowly again to reach a maximum value about one-third of the way into the declining phase. This result is similar to that found at glycinergic synapses (Faber et al., 1992). It is interesting to compare these calculations with experimental observations made on the variability of purinergic quantal currents at the autonomic neuromuscular junction. Recordings of this variability over six EJCs obtained from a visualized varicosity (Fig. 9 *A*) show that the SD of the EJCs also reaches a peak at the time of about one-third decline in the current as in the simulations (compare Fig. 9 *B* with Fig. 8 *C*). Fig. 10 shows the variability in A_2R at the peak of quantal current as the number of receptors increases for a given number of ATP molecules secreted. This variability is given by the SD

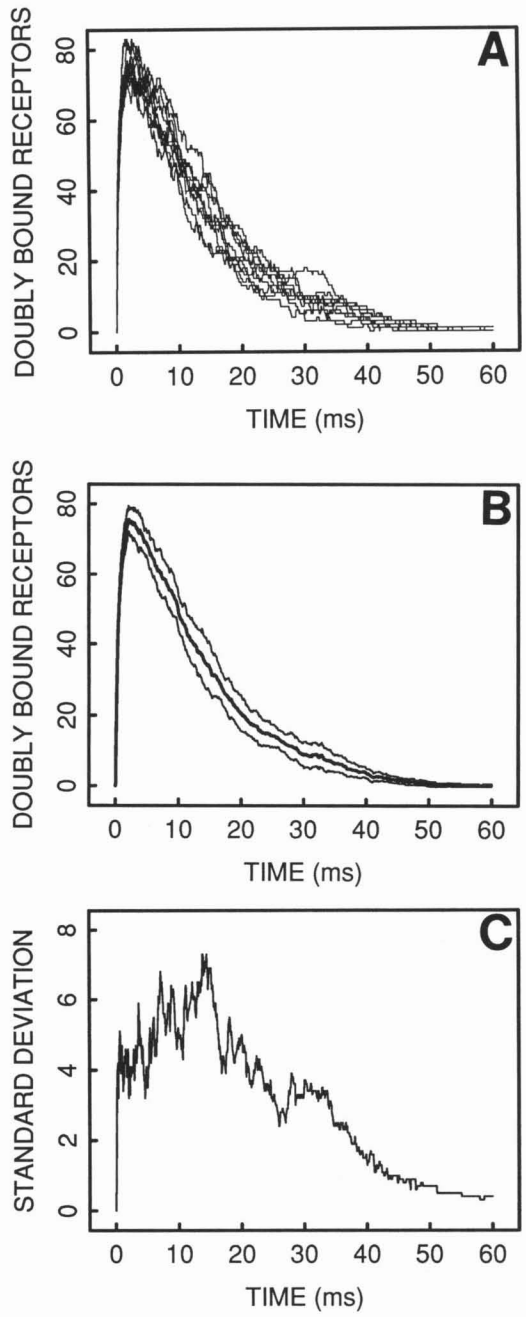

FIGURE 8 Stochastic variation in the quantal response due to 1000 ATP molecules released onto a 0.4-μm^2 receptor patch containing 1000 receptors per μm^2. (*A*) The time course of A_2R for 10 different trials. (*B*) The time course of the mean value of A_2R for 10 different trials (*thick line*), together with upper and lower bounds of 1 SD (*thin lines*). (*C*) SD of the 10 responses in *A*.

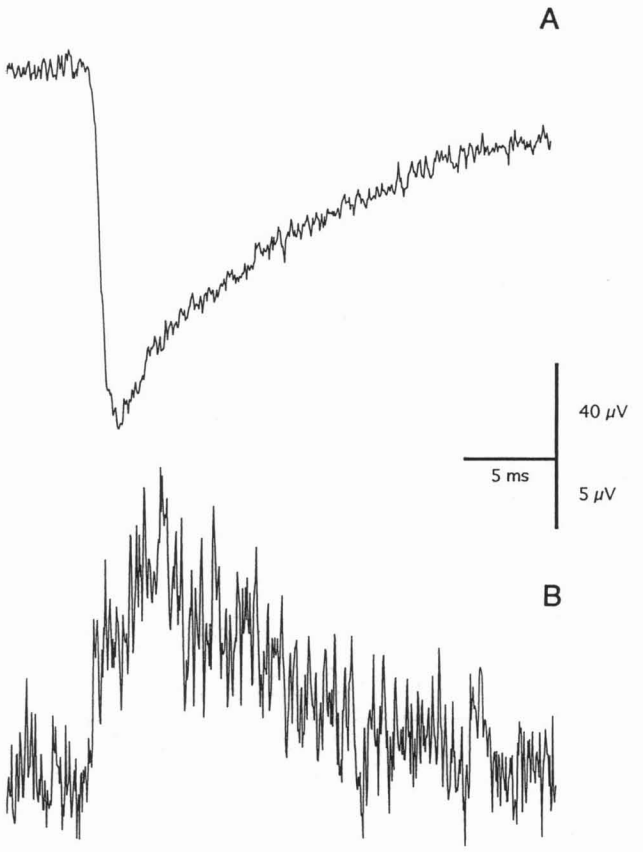

FIGURE 9 Experimental results showing the changes in the variance of the excitatory junctional current due to ATP quanta. (*A*) The average SEJC recorded from a visualized varicosity on the mouse vas deferens (for 6 large SEJCs of about 150 μV); these occurred in a cluster of like-amplitude SEJCs among several such clusters that composed the amplitude-frequency histogram of SEJCs (Fig. 4 *A*). (*B*) SD throughout the EJCs which, after the initial peak during the rising phase of the EJC, increases to reach a maximum during the declining phase of the EJC (compare *B* with Fig. 8 *C*).

bars and decreases as the receptor density increases and also as the number of ATP molecules increases. The coefficient of variation decreases with an increase in receptor density and is smallest for the largest ATP quantum. At 1000 ATP molecules in a quantum and a receptor density of 1000 μm^{-2}, the coefficient of variation is less than 0.1. The variability in the number and spatial distribution of open channels, as well as of doubly bound and singly bound receptors, for different releases of the same number of ATP molecules is shown for three different releases in Fig. 11 *A*. If a single receptor in the middle of the receptor patch is followed for each of these three different releases, then Fig. 11 *B* gives the pattern of stochastic binding of ATP to the receptors (A_2R, AR, and R).

Potentiation of quantal currents due to simultaneous secretion of two packets of ATP

Experiments show that autonomic neuromuscular varicosities can on occasion give spontaneous currents that are more than twice the size of a single quantal current, which has a coefficient of variation of about 0.13 (Bennett, 1994). Such effects have been noted for acetylcholine at the somatic neuromuscular junction by Hartzell et al. (1976) and for glycine at central synapses (Faber and Korn, 1988). The present Monte Carlo model can be used to explore the hypothesis that these large signals result from the simultaneous release of two packets of transmitter and contain potentiation effects arising from the conversion of AR resulting from one packet of ATP to A_2R by the other packet. Fig. 12 *Aa* shows the state

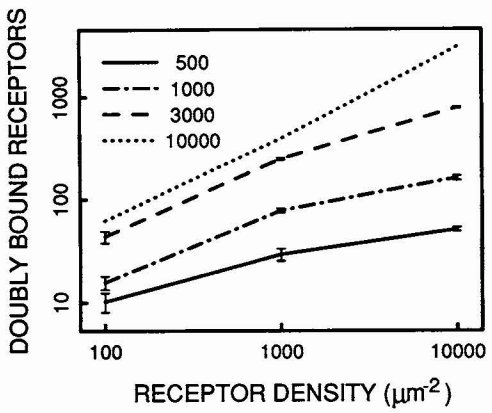

FIGURE 10 Relationship between maximum number of doubly bound receptors (A_2R) and receptor density. Results are shown for several quantal sizes (500 ATP ——; 1,000 ATP – . – . –; 3,000 ATP – – – –; 10,000 ATP · · · · ·). The vertical bars give the SD where they are larger than the thickness of the lines.

of the receptor patch at the peak of A_2R in response to the simultaneous release of two packets of ATP (that is, 2000 molecules). The potentiated increase in A_2R^* that results (about 12%) does not change the time course of A_2R compared with that due to the secretion of a single packet of ATP (Fig. 12 *B*, curves β and δ). In some cases, junctional varicosities have been observed that abut on each other leading to the possibility that if a secretion of ATP occurs from each varicosity at the same time then potentiating effects will occur as a result of ATP diffusing from one varicosity to the receptors beneath an adjacent varicosity; this is illustrated in Fig. 12 *Ab*, where simultaneous releases each of 1000 molecules have been made at the centers of the two adjacent receptor regions. Computations show that a single release of 1000 molecules over one receptor region, but with an adjacent receptor region, gives rise to an increased quantal current above that expected from an isolated varicosity (about 12% more: Fig. 12 *B*, curves γ and δ); again, the time course of this increased current is not much different from that of a single quantal current. Finally, if a packet of ATP is released simultaneously from each of two abutting junctional varicosities, then there is over 30% potentiation in the computed response compared with that due to simultaneous release at two separated varicosities (Fig. 12 *B*, curves α and δ).

Effect of changes in geometry of junctions on time course and amplitude of the quantal current

The amplitude of the quantal current decreases by about 85% when the width of the junction is increased from 50 to 200 nm, and this is similar for receptor areas from 0.1 to 1.0 μm^2 (Table 1). Therefore, if about six or seven varicosities at a distance of 200 nm were to each release a packet of 1000 ATP molecules, the amplitude of the resulting current would be similar to that of a single such ATP packet being released from a varicosity at 50 nm. The time to peak of the quantal current increases with an increase in the junctional width, but does not increase much with an increase in the receptor area (Table 1). Thus, receptor area does not affect markedly the time course of the quantal current.

Effect of ectoenzyme ATPase on the time course of the quantal current

The possibility that an ATPase is located in the junctional cleft and determines the characteristics of the quantal current has not been eliminated by the experiments of Experimental Characteristics of the Quantal Current. Using the kinetics of the ATPase outlined in Materials and Methods, together with an enzyme density of 400 μm^{-2} (which gives a similar ratio of enzyme density/receptor density as found for cholinesterase at the endplate (Bartol et al., 1991)), computations were made of the effects of ATPase. The time course of the quantal current could be maintained in the same range as that observed experimentally if both k_2 and k_{eff} were reduced by a factor of 0.4, which does not change the agreement with Friel (1988) (Fig. 2). If 2000 ATP molecules are released, then the 90% rise time is 1.5 ± 0.3 ms, the τ decay is 21 ± 3 ms, and A_2R peaks at 109 ± 10.

DISCUSSION

A receptor density of 1000 μm^{-2} requires a minimum number of about 1000 molecules of ATP in a released packet to generate about 20 open channels at a junction in less than 2 ms. The vesicle hypothesis identifies the quantum of transmitter with the contents of a synaptic vesicle. The estimate of 1000 ATP molecules in a vesicle is at least an order of magnitude greater than that determined experimentally for small granular vesicles at autonomic neuromuscular junctions. Although the ratio of acetylcholine to ATP in small synaptic vesicles at cholinergic junctions is about 5 (Morel and Meunier, 1981; Israel et al., 1980), giving several thousand ATP molecules in such vesicles, the ratio of noradrenaline to ATP at purinergic junctions appears to be at least 20 (Fried et al., 1984; Fredholm et al., 1982). Because there are only about 1000 molecules of noradrenaline in these small synaptic vesicles, about 50 ATP molecules should be released in a quantum. The large noradrenergic vesicles contain 10,000–16,000 molecules of noradrenaline (Fried et al., 1984); if the ratio of noradrenaline to ATP in these vesicles is about 10:20 (Lagercrantz, 1976; Fried et al., 1984), then up to 1000 ATP molecules may be stored in a vesicle. However, it seems very unlikely that the large synaptic vesicles are the source of the ATP quantum, because there are so few of these vesicles compared with the small synaptic vesicles and they appear to require repetitive stimulation to be released (Kasakov et al., 1988; Whim Lloyd, 1989). An alternative possibility is that ATP and noradrenaline are stored in different small synaptic vesicles; in this case, the stoichiometry estimated in the studies of Lagercrantz and his colleagues may not apply as much to the ratio of noradrenaline to ATP in single synaptic vesicles as to the ratio

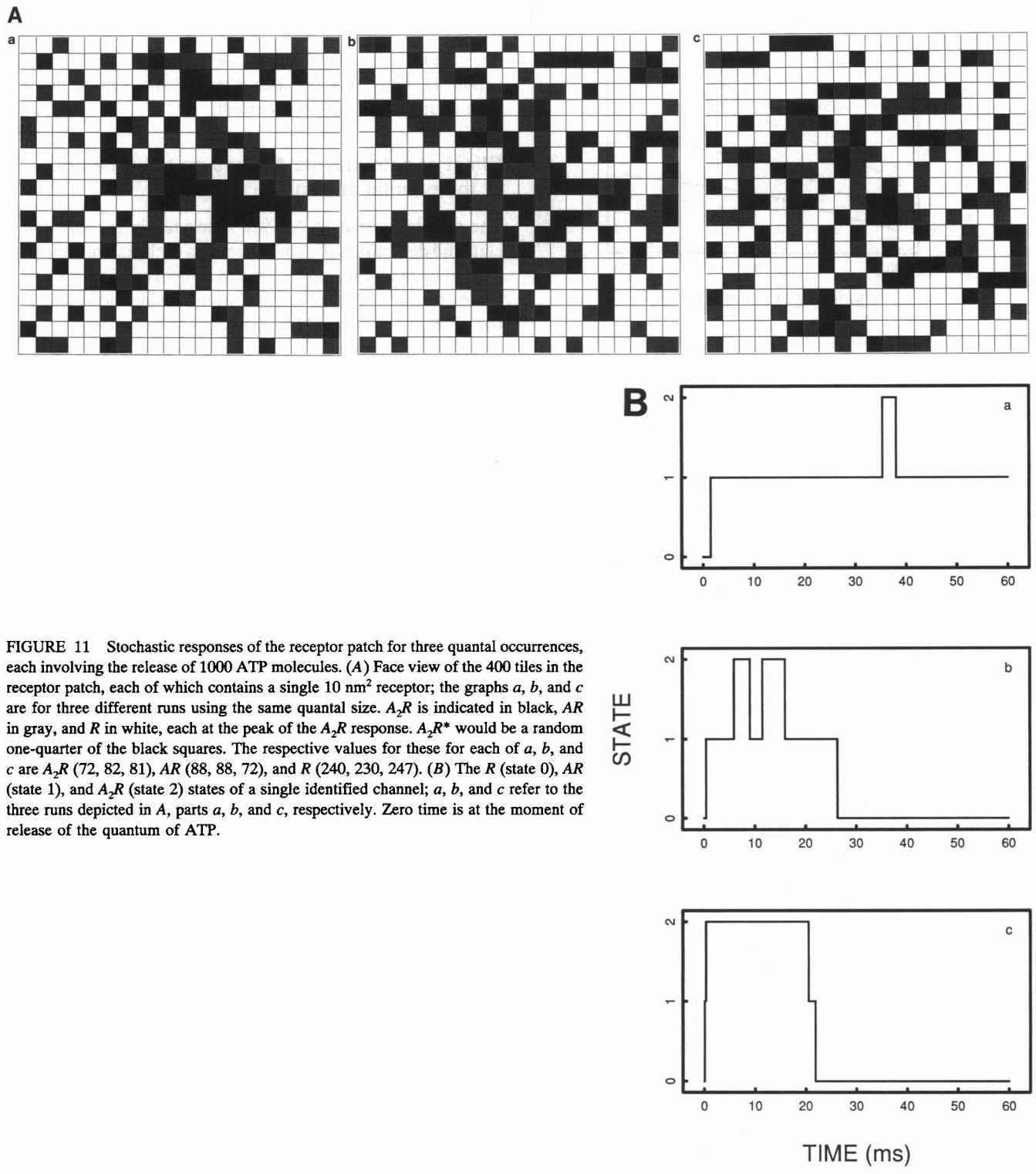

FIGURE 11 Stochastic responses of the receptor patch for three quantal occurrences, each involving the release of 1000 ATP molecules. (*A*) Face view of the 400 tiles in the receptor patch, each of which contains a single 10 nm^2 receptor; the graphs *a*, *b*, and *c* are for three different runs using the same quantal size. A_2R is indicated in black, *AR* in gray, and *R* in white, each at the peak of the A_2R response. A_2R^* would be a random one-quarter of the black squares. The respective values for these for each of *a*, *b*, and *c* are A_2R (72, 82, 81), *AR* (88, 88, 72), and *R* (240, 230, 247). (*B*) The *R* (state 0), *AR* (state 1), and A_2R (state 2) states of a single identified channel; *a*, *b*, and *c* refer to the three runs depicted in *A*, parts *a*, *b*, and *c*, respectively. Zero time is at the moment of release of the quantum of ATP.

of noradrenaline-containing vesicles to ATP-containing vesicles. Indeed, there is some physiological evidence that noradrenaline and ATP may be secreted separately from neuromuscular varicosities (Ellis and Burnstock, 1989).

If about 1000 ATP molecules are secreted in a packet at a junction onto a receptor density of 1000 μm^{-2}, then the number of open channels obtained is about 20 (for $\alpha/\beta = 3$), giving rise to a synaptic current that reaches 90% of its peak value in about 1.4 ms. This density of P_{2x} receptors is an order of magnitude less than that of nicotinic receptors at somatic neuromuscular junctions (Salpeter and Eldefrawi, 1973) and glutamate receptors at central synapses (Harris and Lanellis, 1986). It is not possible for as few as 10 open channels to generate the quantal current without obvious stochastic chan-

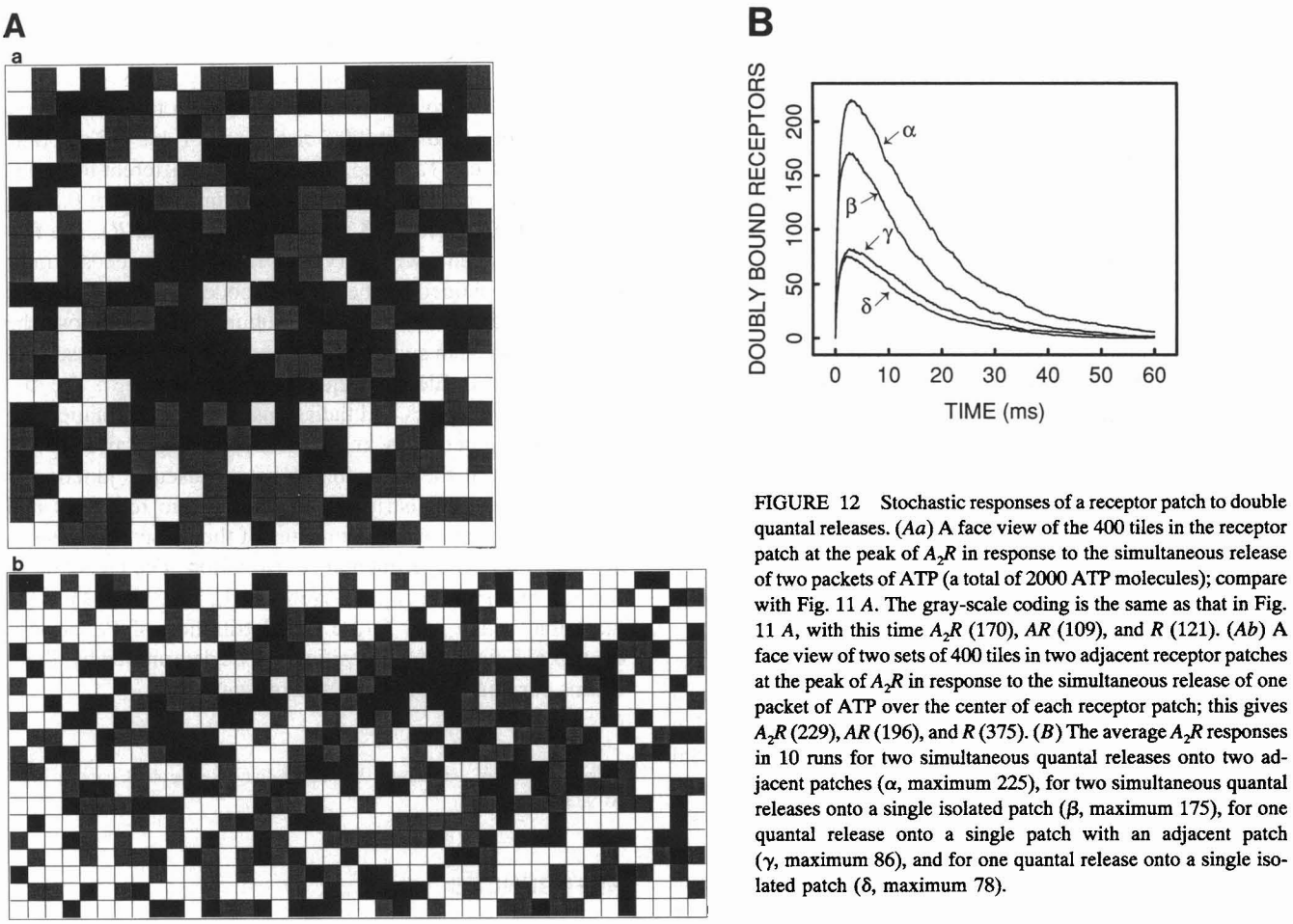

FIGURE 12 Stochastic responses of a receptor patch to double quantal releases. (*Aa*) A face view of the 400 tiles in the receptor patch at the peak of A_2R in response to the simultaneous release of two packets of ATP (a total of 2000 ATP molecules); compare with Fig. 11 *A*. The gray-scale coding is the same as that in Fig. 11 *A*, with this time A_2R (170), AR (109), and R (121). (*Ab*) A face view of two sets of 400 tiles in two adjacent receptor patches at the peak of A_2R in response to the simultaneous release of one packet of ATP over the center of each receptor patch; this gives A_2R (229), AR (196), and R (375). (*B*) The average A_2R responses in 10 runs for two simultaneous quantal releases onto two adjacent patches (α, maximum 225), for two simultaneous quantal releases onto a single isolated patch (β, maximum 175), for one quantal release onto a single patch with an adjacent patch (γ, maximum 86), and for one quantal release onto a single isolated patch (δ, maximum 78).

nel openings occurring in the current record, and this is not observed; 20 channel openings will allow for a reasonably smooth current record. It is interesting to note that about 20 open channels are thought to generate the quantal event at glutaminergic synapses (see, e.g., Edwards et al., 1990). The number of open channels is at least an order of magnitude less than the estimates obtained from the ratio of peak conductance during the junctional current to that of the extrajunctional ATP channel conductance on smooth muscle cells (Finkel et al., 1984). The results suggest that the conductance of purinergic receptors at the junctions is at least an order of magnitude greater than that of the extrajunctional purinergic receptors. In this context, it is interesting to note that extrasynaptic AMPA glutamate receptors appear to have the same conductance as synaptic AMPA glutamate receptors (Hestrin, 1992), whereas extrajunctional acetylcholine receptors on striated muscle cells have a much lower conductance than do the junctional receptors (Miledi et al., 1984).

TABLE 1 Amplitude and time-course of the quantal current: dependence on junctional geometry

Area of junction (μm^2)	Width of junction (nm)	90% rise time (ms)	τ decay (ms)	A_2R peak
0.1	50	1.3 ± 0.5	12 ± 3	44 ± 5
	100	2.1 ± 1.5	9 ± 3	20 ± 5
	200	2.9 ± 2.0	6*	5 ± 2
0.4	50	1.4 ± 0.3	13 ± 2.5	78 ± 4
	100	2.0 ± 0.5	9 ± 2.5	33 ± 6
	200	3.5 ± 0.2	7*	12 ± 3
1.0	50	1.4 ± 0.4	16 ± 2	104 ± 8
	100	2.1 ± 0.5	9 ± 2	52 ± 7
	200	3.1 ± 1.3	9 ± 2	17 ± 3

Entries give the average of 10 runs ± SD, except in the case of two results marked *, where the fluctuations are so great that the value given is an estimate only.

The time course of the quantal current in the mouse vas deferens, recorded with a less than 4-μm-diameter electrode placed over varicosities visualized with the $DiOC_2(5)$ technique, is faster than that recorded with large diameter extracellular recording electrodes. For example, Brock and Cunnane (1988), using large diameter extracellular electrodes of 20 μm or more, recorded quantal currents in the guinea pig vas deferens that had average values of 8 ms for the time to reach 90% of the peak and a 28-ms time constant of decline. These longer times can arise from quantal currents generated by varicosities at the center of the large diameter electrode compared with those due to varicosities at the inside edge (Bennett et al., 1993). The problem can be overcome if small diameter electrodes are placed over a varicosity, although seal resistance itself is still a variable (Stuhmer and Almers, 1982).

The temperature sensitivity of the time course of the junctional current in the guinea pig vas deferens (Cunnane and Manchanda, 1988) may indicate that the action of ATP is inactivated by hydrolysis as well as by diffusion, in much the same way as is acetylcholine at the motor endplate. The ectoenzyme-ATPase and 5′-nucleotidase might be expected to carry out this role, reducing ATP to adenosine in the junctional cleft. However, inhibition of 5′-nucleotidase with AOPCP did not affect the junctional current. The adenosine uptake blocker dipyridamole also had no effect. Furthermore, the ectoenzyme-ATPase inhibitor difluorodinit-robenzene does not potentiate the contractile response of the vas deferens to ATP (Morishita and Furukawa, 1989). Therefore, we have taken diffusion as the main source of inactivation of the transmitter at the junctions. However, to cover the possibility that an ectoenzyme contributes to determining the characteristics of the quantal current, we have considered the effects of an ATPase located in the junctional gap. The effect of this is to require changes in k_2 and k_{eff} for the action of ATP. This then produces results similar to those in the absence of the ectoenzyme.

The possibility that a junctional varicosity can release more than one packet of ATP, both spontaneously and in response to a nerve impulse, has been argued for by Blakeley and his colleagues on the basis of recording multimodal amplitude-frequency histograms of junction potentials thought to arise from a single varicosity (Blakeley et al., 1989). In contrast, Cunnane and Stjärne (1984) have suggested that at most a single packet of ATP is released from a varicosity, either spontaneously or in response to a nerve impulse, and that this saturates the postjunctional receptor patch; in this case, the quantal current is determined by the size of the patch rather than by the amount of transmitter in a packet, as seems to be the case for central synapses (see, e.g., Redman, 1990; Edwards et al., 1990). The argument for monoquantal transmission at varicosities is that because junctional events of like amplitude and time course can be recorded infrequently during long trains of impulses, it is likely that these arise from a single varicosity: this varicosity then secretes a single packet with low probability and gives rise to a characteristically shaped junctional current due to the saturation of receptors beneath the varicosity in question (Astrand and Stjärne, 1988). Table 1 shows that a particular shaped quantal current may be associated with particular varicosities, depending on their distance from the muscle cell membrane. However, the receptor patch is not saturated by the ATP packet according to the present analysis. With a receptor area of 0.4 μm^2 and a receptor density of 1000 μm^{-2}, there are 400 receptors in a patch of which only about 20% are occupied by two ATP molecules at the peak of the junctional current (Table 1).

If two packets of ATP are released simultaneously onto a patch, then the resultant current is about 12% more that that due to two packets released simultaneously onto two separate patches (Fig. 12 *Aa*); this is due to the potentiation effect discussed in Results. A given size packet of ATP may give rise to a characteristically shaped junctional current, both in time course and amplitude (Table 1), but it does not follow that the receptor patch is saturated with ATP. Furthermore, if two packets of ATP are simultaneously released at a distance of 50 nm from a receptor patch, then the time course of the junctional current (90% rise time of 1.4 ± 0.3 ms; time constant of decay 12 ± 1.3 ms) is not very different from that for a single packet of ATP (90% rise time of 1.4 ± 0.3 ms; time constant of decay 13 ± 2.5 ms; see Fig. 12 *B*). The few junctional currents with very long rise times or decay times cannot be explained by the present model. They may be due to the asynchronous release of subunits that compose the SEJC, as has been suggested for such long time course synaptic currents in Electroplaque (Girod et al., 1993). The distribution of receptors and their densities at the somatic neuromuscular junction is known (Salpeter Eldefrawi, 1973), whereas that at the sympathetic neuromuscular junction is not. Whether the distribution of purinergic receptors and their densities arrived at by means of the present analysis is accurate awaits experimental confirmation. The recent cloning of a brain purinoceptor (Webb et al., 1993) holds out the hope that in the near future the distribution of P_{2x} purinoceptors at junctional varicosities will be determined by direct means for comparison with the present work.

This work was supported by Australian Research Council grant AC9330365.

REFERENCES

Astrand, P., and L. Stjärne. 1988. On the secretory activity of single varicosities in the sympathetic nerves innervating the rat tail artery. *J. Physiol.* 409:207–220.

Bartol, T. M., Jr., B. R. Land, E. E. Salpeter, and M. M. Salpeter. 1991. Monte Carlo simulation of miniature endplate current generation in the vertebrate neuromuscular junction. *Biophys. J.* 59:1290–1307.

Bean, B. P. 1990. ATP-activated channels in rat and bullfrog sensory neurones: concentration dependence and kinetics. *J. Neurosci.* 10:1–10.

Bean, B. P., C. A. Williams, and P. W. Ceelen. 1990. ATP-activated channels in rat and bullfrog sensory neurones: current-voltage relation and single channel behaviour. *Neuroscience.* 10:11–19.

Benham, C. M., and R. W. Tsien. 1987. A novel receptor-operated Ca^{2+} permeable channel activated by ATP in smooth muscle. *Nature.* 328: 275–278.

Bennett, M. R. 1994. Quantal secretion from single visualized synaptic varicusities of sympathetic nerve terminals. *Adv. Sec. Messenger & Phosph. Res.* 29:399–424.

Bennett, M. R., W. G. Gibson, and R. R. Poznanski. 1993. Extracellular current flow and potential during quantal transmission from varicosities in a smooth muscle syncytium. *Phil. Trans. R. Soc. Lond. B.* 342:89–99.

Bennett, M. R., P. Jones, and N. A. Lavidis. 1986. The probability of quantal secretion along visualized terminal branches at amphibian (*Bufo marinus*) neuromuscular synapses. *J. Physiol.* 379:257–274.

Blakeley, A. G. H., P. M. Dunn, and S. A. Petersen. 1989. Properties of excitatory junction potentials and currents in smooth muscle cells of the mouse vas deferens. *J. Auton. Nerv. Sys.* 27:47–56.

Brock, J. A., and T. C. Cunnane. 1988. Electrical activity at the sympathetic neuroeffector junction in the guinea pig vas deferens. *J. Physiol.* 399: 607–632.

Burger, R. M., and J. M. Lowenstein. 1970. Preparation and properties of 5′-nucleotidase from smooth muscle of small intestine. *J. Biol. Chem.* 245:6274–6280.

Burnstock, G. 1982. Neurotransmitters and trophic factors in the autonomic nervous system. *J. Physiol.* 313:1–35.

Chabala, L., A. M. Gurney, and H. A. Lester. 1986. Dose-response of acetylcholine receptor channels opened by a flash-activated agonist in voltage-clamped rat myoballs. *J. Physiol.* 371:407–433.

Colquhoun, D., and D. C. Ogden. 1988. Activation of ion channels in the frog end-plate by high concentrations of acetylcholine. *J. Physiol.* 395: 131–159.

Cunnane, T. C., and R. Manchanda. 1988. Electrophysiological analysis of the inactivation of sympathetic transmitter in the guinea-pig vas deferens. *J. Physiol.* 404:349–364.

Cunnane, T. C., and L. Stjärne. 1984. Transmitter secretion from individual varicosities of guinea-pig and mouse vas deferens: highly intermittent and monoquantal. *Neuroscience.* 13:1–20.

Dionne, V. C., J. H. Steinbach, and C. F. Stevens. 1978. An analysis of the dose-response relationships at voltage-clamped frog neuromuscular junctions. *J. Physiol.* 281:421–444.

Dubyak, G. R., and C. El-Moatassim. 1993. Signal transduction via P_2-purinergic receptors for extracellular ATP and other nucleotides. *Am. J. Physiol.* 265:C577–C606.

Edwards, F. A., and A. J. Gibb. 1993. ATP—a fast neurotransmitter. *FEBS Lett.* 325:86–89.

Edwards, F. A., A. J. Gibb, and D. Colquhoun. 1992. ATP receptor-mediated synaptic currents in the central nervous system. *Nature.* 359:144–147.

Edwards, F. A., A. Konnerith, and B. Sakman. 1990. Quantal analysis of inhibitory synaptic transmission in the dentate gyrus of rat hippocampal slices: a patch clamp study. *J. Physiol.* 430:213–249.

Ellis, J. L., and G. Burnstock. 1989. Angiotensiön neuromodulation of adrenergic and purinergic co-transmission in the guinea-pig vas deferens. *Br. J. Pharmacol.* 97:1157–1164.

Evans, R., V. Derkach, and A. Suprenant. 1992. ATP mediates fast synaptic transmission in mammalian neurones. *Nature.* 357:503–505.

Faber, D. S., and H. Korn. 1988. Synergism at central synapses due to lateral diffusion of transmitter. *Proc. Natl. Acad. Sci. USA.* 85:8708–8712.

Faber, D. S., W. S. Young, P. Legendre, and H. Korn. 1992. Intrinsic quantal variability due to stochastic properties of receptor-transmitter interactions. *Science.* 258:1494–1498.

Finkel, A. S., G. D. S. Hirst, and D. F. van Helden. 1984. Some properties of excitatory junction currents recorded from submucosal arterioles of guinea-pig ileum. *J. Physiol.* 351:87–98.

Fredholm, B. B., G. Fried, and P. Hedqvist. 1982. Origin of adenosine released from rat vas deferens by nerve stimulation. *Eur. J. Pharmacol.* 79:233–243.

Fried, G., H. Lagercrantz, R. Klein, and A. Thureson-Klein. 1984. Large and small noradrenergic vesicles—origin, contents and functional significance. *In* Catecholamines: Basic and Peripheral Mechanisms. Alan R. Liss, New York. 45–53.

Friel, D. D. 1988. An ATP sensitive conductance in single smooth muscle cells from the rat vas deferens. *J. Physiol.* 401:361–380.

Friel, D. D., and B. P. Bean. 1988. Two ATP-activated conductances in bull frog atrial cells. *J. Gen. Physiol.* 91:1–27.

Girod, R., P. Corréges, J. Jacquet, and Y. Dunant. 1993. Space and time characteristics of transmitter release at the nerve-electroplaque junction of Torpedo. *J. Physiol.* 471:129–157.

Gordon, E. L., J. D. Pearson, and L. L. Slakey. 1986. The hydrolysis of extracellular adenine nucleotides by cultured endothelial cells from pig aorta. *J. Biol. Chem.* 261:15496–15504.

Harris, K. M., and D. M. D. Lanellis. 1986. Membrane structure at synaptic junctions in area CA1 of the rat hippocampus. *Neuroscience.* 19:857–872.

Hartzel, H. C., S. W. Kuffler, and D. Yoshikami. 1976. Postsynaptic potentiation: neuromuscular synapse. *J. Physiol.* 251:427–463.

Hestrin, S. 1992. Activation and desentization of glutamate-activated channels mediating fast excitatory synaptic currents in the visual cortex. *Neuron.* 9:991–999.

Hirst, G. D. S., N. J. Bramich, F. R. Edwards, and M. Klemm. 1992. Transmission at autonomic neuroeffector junctions. *Trends Neurosci.* 15:40–46.

Israel, I., R. Manaranche, J. Marsal, F. M. Meunier, N. Morel, P. Frachon, and B. Lesbats. 1980. ATP-dependent calcium uptake by cholinergic synaptic vesicles isolated from Torpedo electric organ. *J. Membr. Biol.* 54:115–126.

Kasakov, L., J. Ellis, K. Kirkpatrick, P. Milner, and G. Burnstock. 1988. Direct evidence for concomitant release of noradrenaline, adensoine 5′-triphosphate and neuropeptide from sympathetic nerve supplying the guinea-pig vas deferens. *J. Auton. Nerv. Sys.* 22:75–82.

Klemm, M. 1993. Structure of specialized neuromuscular junctions in the longitudinal muscle of the guinea-pig ileum. *Proc. Aust. Neurosci. Soc.* 4:80.

Kuffler, S. W., and D. Yoshikami. 1975. The numbers of transmitter molecules in a quantum: an estimate from ionophorectic application of acetylcholine at the neuromuscular synapse. *J. Physiol.* 251:465–482.

Lagercrantz, H. 1976. On the composition and function of large dense cored vesicles in sympathetic nerves. *Neuroscience.* 1:81–92.

Land, B. R., W. V. Harris, E. E. Salpeter, and M. M. Salpeter. 1984. Diffusion and binding constants for acetylcholine derived from the falling phase of miniature endplate currents. *Proc. Natl. Acad. Sci. USA.* 81: 1594–1598.

Lavidis, N. A., and M. R. Bennett. 1992. Probabilistic secretion of quanta from visualized sympathetic varicosities in mouse vas deferens. *J. Physiol.* 454:9–26.

Miledi, R., G. Reiser, and O. D. Uchitel. 1984. Characteristics of membrane channels induced by acetylcholine at frog muscle-tendon junctions. *J. Physiol.* 350:269–277.

Morel, N., and F. M. Meunier. 1981. Simultaneous release of acetylcholine and ATP from stimulated cholinergic synaptosomes. *J. Neurochem.* 36: 1766–1773.

Morishita, H., and T. Furukawa. 1989. Low calcium and calcium antagonists potentiate the contraction of guinea-pig vas deferens induced by ATP: a permissive role for P_2-purinoceptors. *Eur. J. Pharmacol.* 164:507–513.

Nagy, A. 1986. Enzymatic characteristics and possible role of synaptosomal ecto-adenosine triphosphatase from mammalian brain. *In* Cellular Biology of Ectoenzymes. G. Kreutzberger, M. Reddington, and H. Zimmerman, editors. Springer Verlag, Berlin. 49–57.

Parnas, H., M. Flashner, and M. E. Spira. 1989. Sequential model to describe the nicotinic synaptic current. *Biophys. J.* 55:875–884.

Redman, S. 1990. Quantal analysis of synaptic potentials in neurones of the central nervous system. *Physiol. Rev.* 70:165–198.

Salpeter, M. M., and M. E. Eldefrawi. 1973. Size of endplate compartments, density of acetylcholine receptors and other quantitative aspects of neuromuscular transmission. *J. Histochem. Cytochem.* 21:769–778.

Silinsky, E. M., V. Gerzanich, and S. M. Vanner. 1992. ATP mediates excitatory synaptic transmission in mammalian neurones. *Br. J. Pharmacol.* 106:762–763.

Sneddon, P., and G. Burnstock. 1984. Inhibition of excitatory junction potentials in guinea-pig vase deferens by α, β-methylene ATP: further evidence for ATP and noradrenaline as co-transmitters. *Eur. J. Pharmacol.* 100:85–90.

Sneddon, P., and D. P. Westfall. 1984. Pharmacological evidence that adenosine triphosphate and noradrenaline are co-transmitters in the guinea-pig vas deferens. *J. Physiol.* 347:561–580.

Stuhmer, W., and W. Almers. 1982. Photobleaching through glass micropipettes: sodium channels without lateral mobility in the sarcolemma of frog skeletal muscles. *Proc. Natl. Acad. Sci. USA.* 79:946–950.

Wathey, J. C., M. M. Nass, and H. A. Lester. 1979. Numerical reconstruction of the quantal event of nicotinic synapses. *Biophys. J.* 27:145–164.

Well, T. E., J. Simon, B. J. Krishek, A. N. Bateson, T. G. Smart, B. F. King, G. Burnstock, and E. A. Barnard. 1993. Cloning and functional expression of a brain G-protein-coupled ATP receptor. *FEBS Lett.* 324:219–225.

Whim, M. D., and P. E. Lloyd. 1989. Frequency-dependent release of peptide cotransmitters from identified cholinergic motor neurons in Aplysia. *Proc. Natl. Acad. Sci. USA.* 86:9034–9038.

Wu, P. H., and J. W. Phillis. 1984. Uptake by central tissues as the mechanism for the regulation of extracellular adenosine concentrations. *Neurochem. Int.* 6:613–632.